Seismic Response Control of Offshore Platforms Equipped with Optimum Localization of SMA

Mohammad Aghajani Delavar[1a] and Khosrow Bargi[*1]

[1]School of Civil Engineering, College of Engineering, University of Tehran, Iran

Abstract. In this paper, the seismic response control of offshore jacket-type platform equipped with Shape Memory Alloy (SMA) braces is investigated. Concerning the properties of the SMAs, a new connection is introduced in order to make the most of it. Based on an actual platform structure and its mechanical model, the optimized localization of SMAs are found by damage propagation under pushover loadings. To evaluate the possibility of adopting the innovative bracing system and its efficiency, the dynamic responses of 3-D model of the existing 4-legged offshore platform placed in Persian Gulf (SPD12) is compared to the ones with SMA braces. The results show that using an SMA element is an effective way to develop the API recommendations and improve the dynamic response of offshore platforms subjected to earthquake excitations. Implementing the SMA braces can lead to a reduction in residual displacement, deck level displacement, elements and connections forces, and base shear compared to the steel tubular braces model.

Keywords: platform, SMA, seismic assessment, offshore, jacket, SMA connection

1. Introduction

Offshore platforms should be safe and comfortable to guarantee the living and working conditions of workers. However, many offshore platforms have been installed in seismic regions and can be damaged easily by earthquakes. Therefore, controlling the structure under seismic loading needs to be conducted. The seismic control of the fixed jacket-type offshore platforms can be useful to reduce the required construction materials volume, increase the service life, and improve the reliability of the structure under seismic loads and oscillations. There are many methods for the control of structures subjected to earthquake-induced loads, but the application of these methods needs to be considered and assessed for offshore structures. One innovative method which is not mainly considered in offshore platforms yet is utilizing Shape Memory Alloys (SMAs) to control these structures under seismic loading.

The Nitinol (which is very common SMA type) is a kind of intelligent material that can undergo large recoverable strains of about 6-9% without any plasticity [1,2]. SMAs are effective material for seismic application due to good fatigue resistance, long-term reliability even after strong earthquakes, high damping capacity, and the recovery of strains [3-6]. Many researchers have studied using SMAs in seismic control of buildings and bridges. Asgarian and Moradi [7] investigated the seismic performance of steel frames equipped with SMA braces. Wilde et al [8] assessed base isolation system with shape memory device for elevated highway bridges that could control the displacements of the rubber bearing. A critical review for the applications of using SMAs in seismic resistant design is provided by Desroches and Smith [9]. Tamai et al [10] investigated the application of SMA rod to

[*] Correspondence author, Email: kbargi@ut.ac.ir, Tel: +989121128923

exposed-type column base experimentally and analytically. Haque and Alam [11] investigated the feasibility of the novel piston-based self-centering bracing (PBSC) system and predicted its load-deformation hysteresis during seismic events. Some researchers are studied on steel structures connections using SMAs [12-16]. On the other hand, assessment of jacket-type platforms equipped with SMAs has seldom been studied. Li et al [6] investigated the seismic control of offshore platform structures with SMA dampers and found that the SMA damper is an effective control device for these structures. Shabakhty and Givkay [17] used SMA braces to control the response of fixed offshore platforms under extreme wave loading, and Aghajani Delavar et al. [18] did similar research under seismic loading, but they didn't present any optimum and practical method to use SMAs in braces. In this research, the seismic response behavior of fixed jacket-type offshore platforms equipped with SMAs being used in optimum locations is investigated and compared with the ones without SMAs, and a practical method for applying the SMAs to the brace elements is proposed.

2. FE modeling and analysis

2.1 Details of the case study

In this research, a 3-D model of SPD12 jacket-type platform located in Persian Gulf is selected as a case study. The jacket which is fixed to the ground by 4 piles has four main legs located in 71.4-meter water depth. The top side of the platform is 20.50m×24.25m and consists two distinguished parts; main module and Free Water KO drum module (FWKO module). The main module has four decks, and the FWKO module has three decks. Mudline elevation of the platform has 33.25m×38.50m plan dimension. General configuration of SPD12 jacket platform is shown in Fig.1.

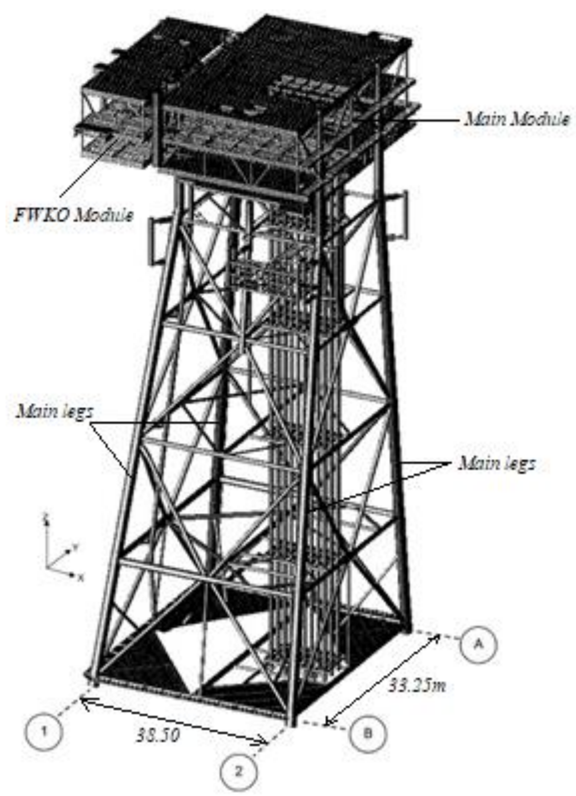

Fig. 1 Perspective plot of SPD12 jacket platform [19]

2.2 Modeling of the jacket

Considering the effects of hydrodynamic forces and added mass are essential to model the tubular members of the jacket. Therefore, the buoyancy forces (effect of hydrodynamic forces) and the simplified added mass (calculated by the added mass coefficients) are assigned to the model. Computer model is created using the SAP2000 software [20] which is more powerful in analyzing such an intricate model than other software and useful for modeling of tubular members and assignments of nonlinear behavior of elements due to its user-friendly modeling.

In dynamic analysis, the mass should contain the mass of the platform associated with gravity loading including the platform dead weight, actual live loads and 75% of the maximum supply and storage loads [21]. Moreover, additional moment due to P-Δ effects is considered because the vertical load in this structure is large.

For modeling of the jacket-type platform, the properties of steel are presented in Table 1. Table 2 indicates the yield stress of the steel considering the thickness of the tubular elements. Bilinear stress-strain curve with 3% of the elastic slope and maximum ductility of 14 is modeled for considering the material non-linearity (Fig. 2). The elements are beam-column due to the loading assignment to be more similar to the SPD12, and all the connections are moment resistant which are simulated as the real structure. The 5% damping ratio is considered for this simulation.

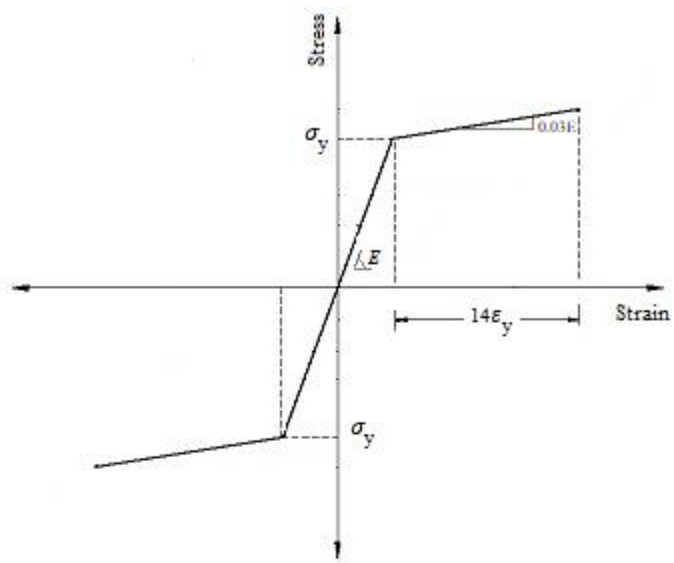

Fig. 2. Steel material

Table 1. Steel properties

Grade	Density	Young's Modulus	Poisson's Ratio
S355	7850 kg/m^3	200 GPa	0.3

Table 2. Yield stress of steel (N/mm^2)

Thickness in mm					
≤16	>16	>40	>63	>80	>100

	≤40	≤63	≤80	≤100	≤150
350	345	335	325	315	295

2.3 Modeling of the interactions

During the analysis of jacket-type offshore platforms simplified methods can be used to obtain the effects of interactions; soil-pile interaction and water-structure interaction, provided that the purpose of analysis is the study of global behavior of the structure. The main object of this article is the comparison of seismic responses with and without using of SMAs in the platforms relatively. Therefore, for considering the soil-pile interaction, the equivalent length method is used. The equivalent length of the pile in loose clayey soils is suggested 8D-12D, where D is the diameter of the pile [22]. In this research, the value of 12D which is approximately equal to 18.3m is considered as the equivalent length of piles. For considering the water-structure interaction, the added mass coefficient is used to assign the calculated added mass to the elements. The added mass coefficients as a function of submergence are presented in Fig. 3 and Table 3. When the tubular element is fully submerged (*d*>*D*), the value for the vertical added mass coefficient is the same as that for the horizontal one [23].

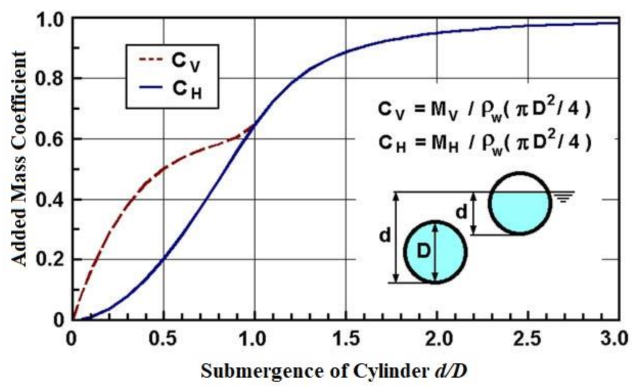

Fig. 3 Vertical and horizontal added mass coefficients of cylinder as a function of submergence ratio *d/D* [23]

Table 3 Buoyancy and added mass coefficients of cylinder [23]

Submergence ratio d/D	Buoyancy/ $\rho_w gA$ where $A=\pi D^2/4$	Added mass coefficient	
		Vertical $C_V = M_V/\rho_w A\ddot{u}_z$	Horizontal $C_H = M_H/\rho_w A\ddot{u}_x$
0.1	0.052	0.163	0.009
0.2	0.142	0.286	0.036
0.5	0.500	0.500	0.203
0.8	0.858	0.581	0.461
1.0	1.000	0.646	0.646
1.2	1.000	0.783	0.783
1.5	1.000	0.885	0.885
2.0	1.000	0.948	0.948
3.0	1.000	0.983	0.983

2.4 Modeling of the topside

In assessing the jacket part, modeling the topside (deck) with precise details is not necessary. Thus, a simplified model is used to consider the real height of the structure. To do so, the columns are modeled, and membrane elements which are suitable in distribution of gravitational load are chosen to model the deck. Each deck is modeled as an independent diaphragm in order to have the ability to move relatively.

2.5 Modeling of the SMAs

Over the past decades, constitutive models have been proposed by several researchers for capturing the behavior of the SMAs. In this paper, a constitutive model proposed by Fugazza [24] was selected to represent the super-elastic behavior of the SMAs. This kind of constitutive model can be simulated easily due to the few parameters it required. These parameters are the austenite to martensite starting stress (σ_s^{AS}), the austenite to martensite finishing stress (σ_f^{AS}), the martensite to austenite starting stress (σ_s^{SA}), the martensite to austenite finishing stress (σ_f^{SA}), modulus of elasticity for austenite and martensite phases (E^{SMA}) and the super-elastic plateau strain length (ε_L). The hysteresis loop of an SMA element looks like a flag that has the benefit of some energy dissipation along with minimal residual deformations upon removal of loads. Fig. 4 represents the SMA model schematically which has no strength degradation during cycling, and the martensite and austenite modulus of elasticity are the same [25,26]. The mechanical behavior of the SMAs are provided in Table 4 which is based on the uniaxial cyclic tests carried out by DesRoches et al [27].

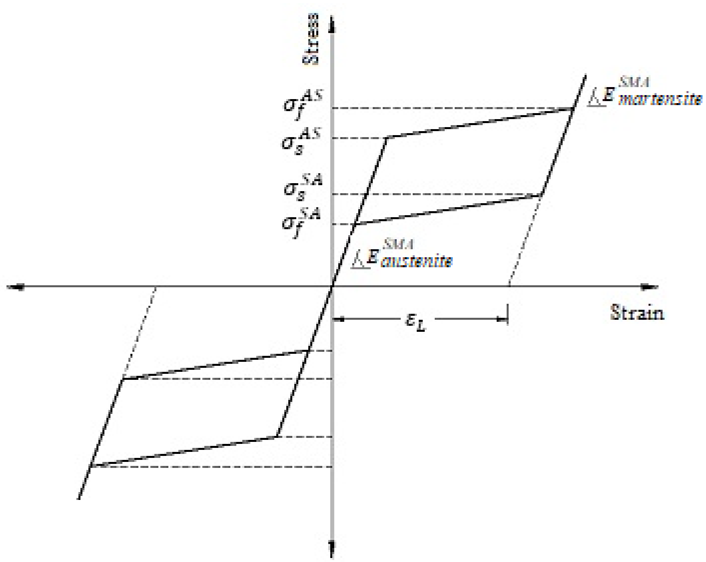

Fig. 4 Stress-strain relationship of SMA member: parameters needed for the model

Table 4 Mechanical properties of SMA bars in numerical simulation

Quantity	E^{SMA}	σ_s^{AS}	σ_f^{AS}	σ_s^{SA}	σ_f^{SA}	ε_L
Value	27579 MPa	414 MPa	550 MPa	390 MPa	200 MPa	3.5%

For modeling the super-elastic SMA behavior in SAP2000, multiple link elements can be used. By defining two link properties and assign them to two link elements in parallel, the SMA behavior can be obtained. A multi-linear plastic link utilizing the pivot model is used to define the hysteresis loop, and a multi-linear elastic link is used to shift the hysteresis loop away from the origin. Fig. 5 shows the modeling of SMA element in SAP2000 in comparison to DesRoches's model which is verified by experimental works.

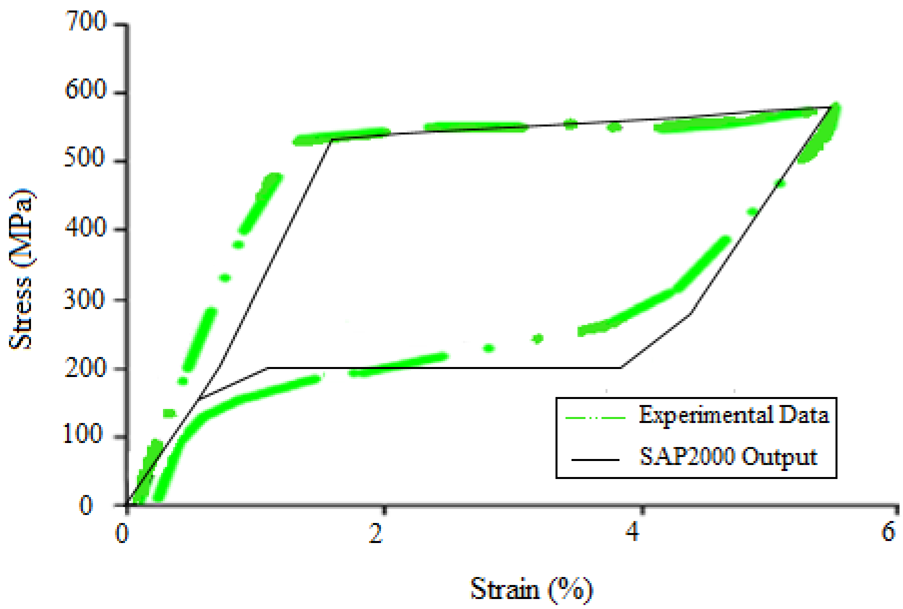

Fig. 5 Verifying SMA modeling in SAP2000 with DesRoches model

2.6 Modal analysis

A modal analysis is conducted to extract the mode shapes of the structure and the corresponding periods with considering P-Δ effect. Fig. 6 shows the first three mode shapes of the SPD12. As shown in Table 5, first 12 periods of the generated model are compared with the corresponding period of the structure. The first two periods of the structure are very similar to their corresponding generated model and other periods have about 10% variation in average due to the simplification of the model.

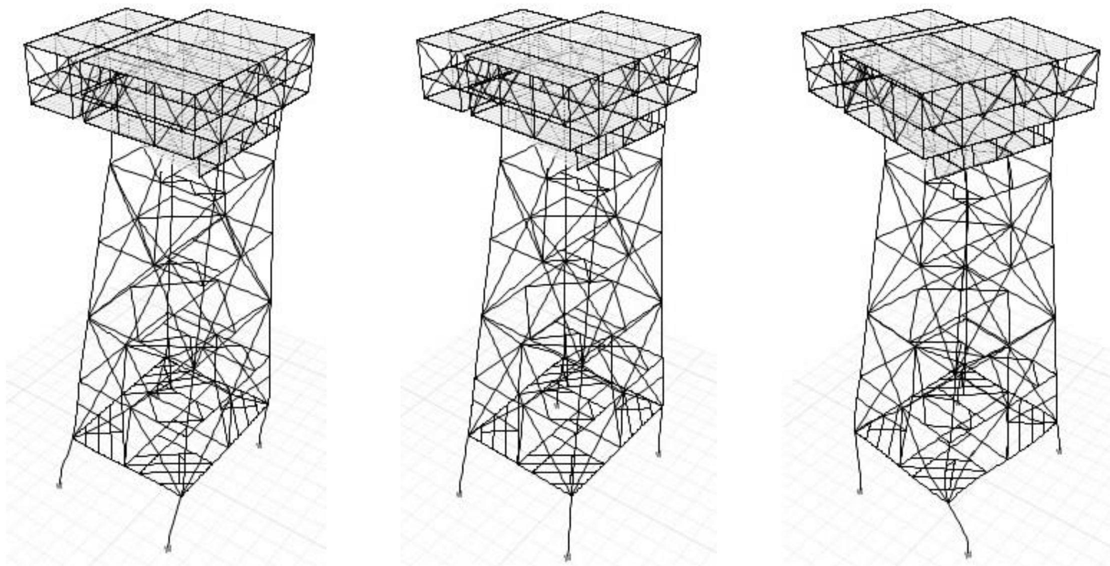

a) Mode-1 b) Mode-2 c) Mode-3

Fig. 6 Mode Shapes of the platform

Table 5 Comparison of periods

Mode	Modal Period	SPD12 Period	Error (%)
1	2.957	3.004	1.5
2	2.506	2.565	2.3
3	2.081	1.638	-27.0
4	1.179	0.974	-21.0
5	1.145	0.945	-21.0
6	0.738	0.739	0.1
7	0.455	0.533	14.6
8	0.415	0.531	21.8
9	0.403	0.500	19.4
10	0.341	0.341	0.0
11	0.292	0.308	5.2
12	0.279	0.286	2.4

2.7 Pushover analysis

Nonlinear static analysis is conducted to obtain the damage propagation in the structure to find places where the structure will be damaged first. Thus, defining hinges for all the main elements of the SPD12 is done and the structure is pushed with two kinds of loading; modal and constant pattern distribution of load.

Due to the fully restrained moment frames and concentric braced frames of the platform, calculating parameters and numerical acceptance criteria for beams, columns, and braces are obtained with respect to FEMA [28] and Iranian code number 360 [29] to define hinges for nonlinear analysis. Due to the forces and configuration of the elements, component actions might be Deformation-Controlled (DC) or Force-Controlled (FC). Characteristics of the sections (like t/D) cause the columns and most of the beams to be FC. By the pushover analysis, the initial elements that experience the collapse prevention (CP) are braces which are DC. As a result, damage distribution of each frame is obtained and using SMAs for controlling the seismic response of the structure can be optimized by this method.

By conducting push over analysis, plastic hinges are formed in braces first, then spread to the other members which are investigated by Aghajani Delavar and Bargi [30]. The collapse spread process provides the opportunity to recognize the next potential member in which the plastic hinges may be formed. This would result in finding optimum places to reinforce the structure. According to the analysis, braces are those members.

2.8 Design of SMA braces

For comparing the two structures which are SPD12 platform with and without SMA braces, super-elastic SMA braces are designed to provide the same yielding strength and the same axial stiffness as tubular steel braces. Therefore, cross section and length of the SMA elements (A^{SMA}, L^{SMA}) can be obtained [8]. To do so, the following relations are achieved:

$$A^{SMA} = \frac{F_y}{\sigma_s^{AS}} = \frac{f_y^{steel} \times A^{steel}}{414} = \frac{(355\ or\ 345)A^{steel}}{414} = \begin{matrix} 0.857A^{steel} \\ 0.833A^{steel} \end{matrix}$$

$$L^{SMA} = \frac{E^{SMA} \times A^{SMA}}{K^{steel}} = \frac{27579 \times A^{SMA}}{2 \times 10^5 \times A^{steel} / L^{steel}} = \begin{matrix} 0.118L^{steel} \\ 0.115L^{steel} \end{matrix}$$

As the SMA bars are made in small diameter, they cannot resist compression forces and can buckle simply, so SMA bars should be tensile elements. For modeling of the SMA braces due to the length and the cross section of needed SMAs, these braces are modeled with SMA which has the required stiffness and is in compliance with force-displacement curve. The link elements which are defined in SAP2000 have independent configurations that the length and the cross section of the SMA is considered in its P-Δ curve, so drawing with different length didn't make any difference in modelling. For solving the problem of the SMA bars in compression forces, new connection of SMA to the steel braces is introduced which makes SMA elements be in tension although the brace is in compression. As a result, Symmetric P-Δ curve (Fig. 5) is used to consider the compression part as same as the tension one for modeling the SMA elements.

2.9 Proposed connection between SMA and tubular braces

One of the objectives of this article is utilizing the SMA behavior, especially having no residual strain, in offshore platforms. Due to not being capable of restricting SMA bars under the compression forces, the SMA braces should design in such both tension and compression. Fig. 7 presents the proposed connection in SMA braces. This novel connection is inspired from the conducted research by Kari [31] who proposed a constitutive SMA braces in BRB frames.

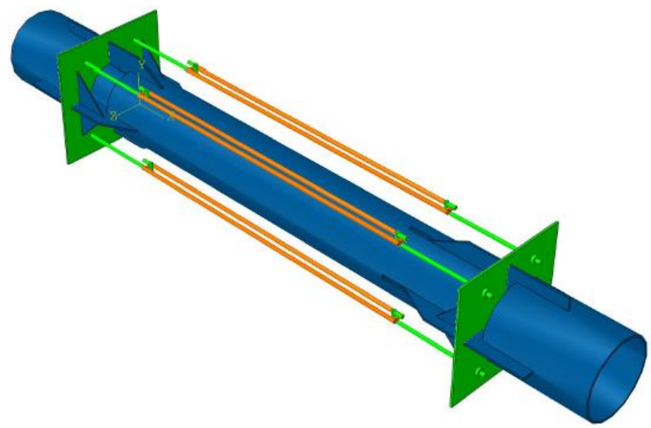

(a)

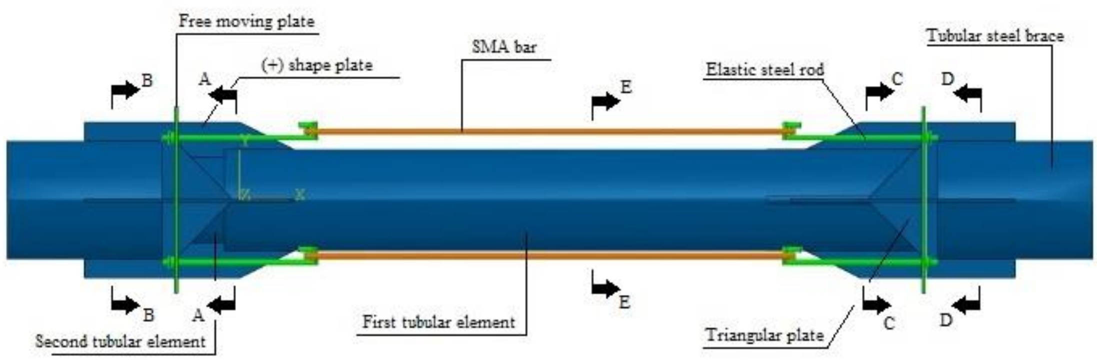
Free moving plate
(+) shape plate
SMA bar
Elastic steel rod
Tubular steel brace
B
A
E
C
D
Second tubular element
First tubular element
Triangular plate

(b)

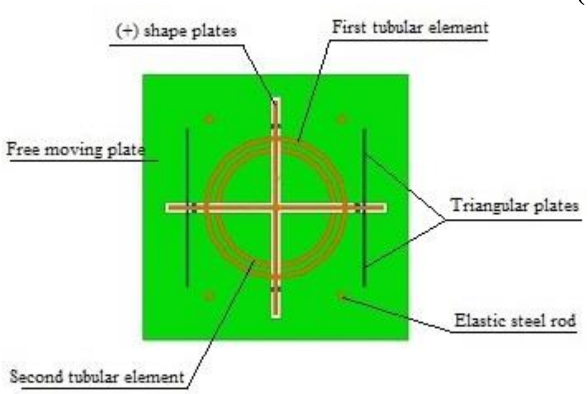
(+) shape plates
First tubular element
Free moving plate
Triangular plates
Elastic steel rod
Second tubular element

(c)

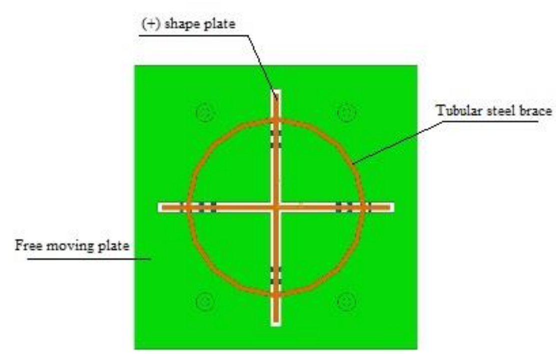
(+) shape plate
Tubular steel brace
Free moving plate

(d)

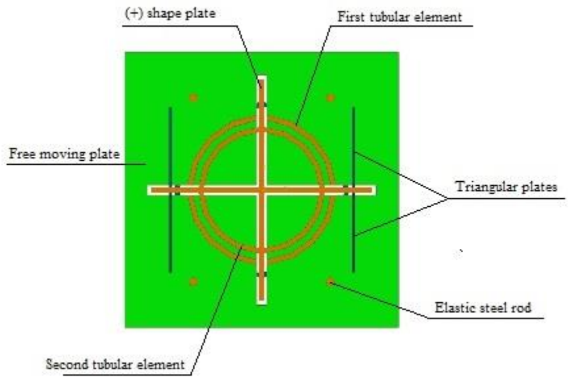

(e)

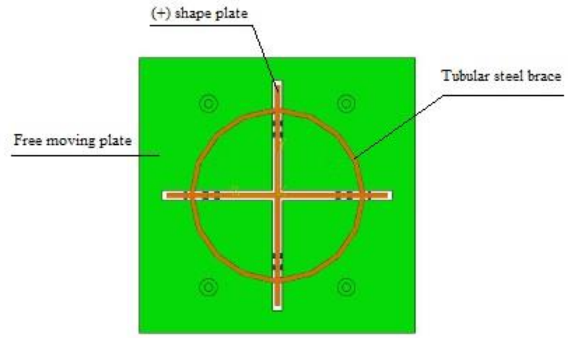

(f)

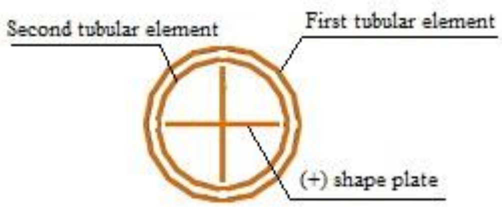

(g)

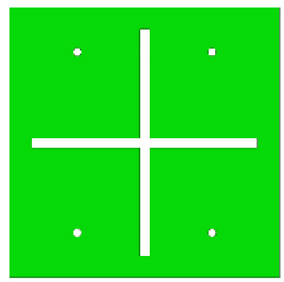

(h)

Fig. 7 Details of the proposed connection; (a) 3-D model, (b) 2-D model, (c) Section A-A, (d) Section B-B, (e) Section C-C, (f) Section D-D, (g) Section E-E, and (h) Free moving plate

As shown in Fig. 7, this SMA brace consists of tubular steel and SMA elements. The SMAs are connected to the main tubular elements in such a way that the SMAs are under tension forces. For obtaining this purpose, some plates and two short tubular elements which have different diameter are considered. First tubular element is connected to the left side of the main tubular brace and its right side is free to move, and second one is connected to the right side of the main tubular brace and its left side is free to move. The SMA bars are connected to the plates which are free to move in axial direction of the brace. When the brace is under tension, the two triangle plates push the moving plates apart from each other and the SMA bars will experience the tension. When the brace is under compression, the two short tubular elements push the moving plates from their free sides, so the SMA bars will be under tension again.

2.10 Non-linear time history analysis

For time history analysis, the appropriate earthquake records of the location of the structure are better to be provided. The ground displacement, ground velocity, or ground acceleration are the forms of lateral loadings that earthquake records should be applied. Unfortunately, earthquake records from the considered region were not available to be used in this research. In this paper, earthquake acceleration records, which are provided by the University of Berkley database, used are El Centro/US, Kobe/Japan, and Tabas/Iran earthquakes to compare the effect of SMAs on the considered structure. The details of these ground motions can be seen in Table 6 and Fig. 8. To apply the selected accelerograms for the time history analyses, they are scaled to the maximum acceleration of the region which is 0.35g with respect to the SeismoSignal software [32]. Each record is applied at the fixity level of the equivalent piles as a horizontal component. The earthquakes are applied in both directions (X and Y) separately and the results are obtained to compare these structures.

Table 6 Details of the ground motions

Earthquake	Year	Peak Ground Accelerating (g)	Time step (s)	Duration (s)
El Centro	1940	0.291	0.01	53.71
Kobe	1995	0.309	0.01	31.99
Tabas	1978	0.968	0.02	32.98

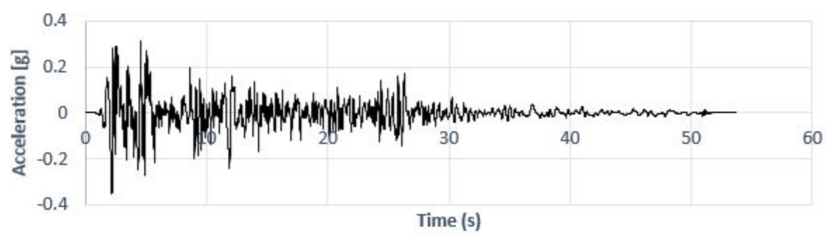

(a)

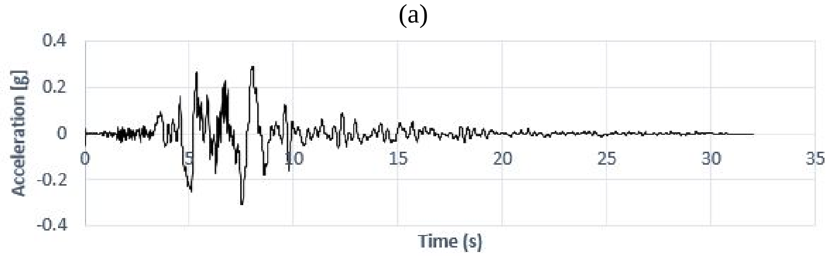

(b)

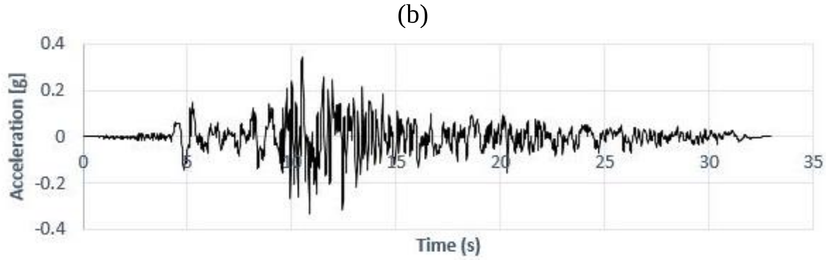

(c)

Fig. 8 Earthquake acceleration records; (a) ElCentro, (b) Kobe, and (c) Tabas

3. Results

Pushover analysis and non-linear time history analysis are conducted on two main types of structure; SPD12 with tubular steel braces and SPD12 with SMA braces. The SPD12 with SMA braces is sorted by 4 kinds of structure; SPD12 with SMA braces in 3rd level, SPD12 with SMA braces in 1st level, SPD12 with SMA braces in 1st and 3rd levels, and SPD12 with SMA braces in all levels which are presented in Fig. 9. The reason of selecting 1st and 3rd level is due to the damage propagation in SPD12 under modal or constant pattern distribution pushover loading. For modal pattern distribution loading, damages are initiated from 3rd level, and for constant one, damages are initiated from 1st level. Thus, 1st and 3rd levels are vulnerable to be damaged.

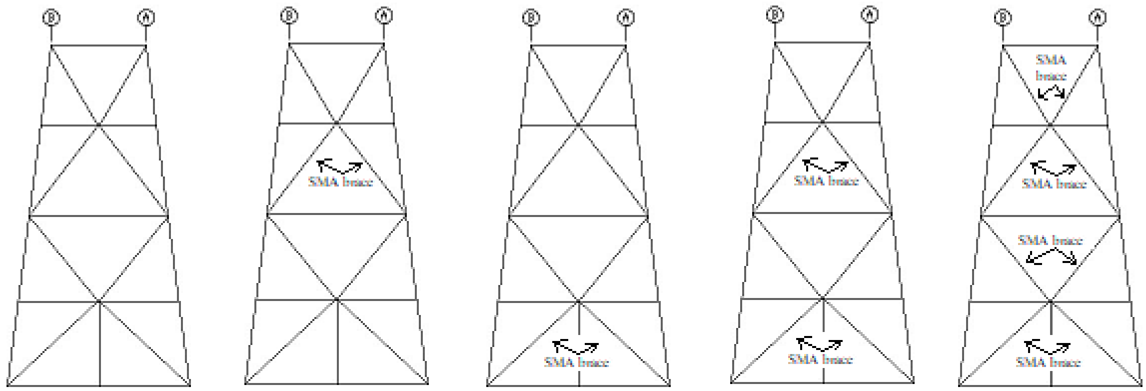

(a) (b) (c) (d) (e)

Fig. 9 Types of SPD12 in modeling; (a) with tubular steel braces. (b) with SMA braces in 3rd level, (c) with SMA braces in 1st level, (d) with SMA braces in 1st and 3rd levels, and (e) with SMA braces in all levels

3.1. The effect of SMA braces on internal forces of the structure

For assessing the internal forces in the platform and comparing the effect of the SMA braces, one brace of the jacket platform is modeled independently which is shown in Fig. 10. For assessing the SMA braces, three kinds of elements are modeled; tubular steel, element with combination of tubular steel and SMA (SMA braces), and SMA element. These models are subjected to displacement loading and have the same stiffness. The maximum bearing forces are presented in Table 7.

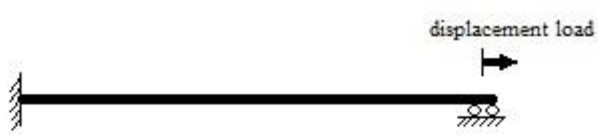

Fig. 10 Modeling of brace element

Table 7 Maximum bearing forces (kN) of elements under displacement loading of 0.167m

Modeling type	Maximum bearing force
Tubular steel	56160
SMA brace	9649
SMA in total length	10180

As shown in Table 7, the internal forces of the brace element will be reduced about 85% by considering the SMA bars. As a result, stress in the elements and the connections will be reduced which confirms the research studied by Shabakhty and Givkay [18], and utilizing SMA bars leads delay the structure collapse.

The internal forces in SMA brace and SMA in total length are approximately the same which confirms the modeling of the whole platform with SMA in total length instead of SMA braces for simplifying the calculations.

3.2. The effect of SMA braces on the displacement of the deck level and base shear

The time histories of displacement of the deck level subjected to the accelerograms of El Centro, Kobe, and Tabas are presented in Fig. 11 for the five types of SPD12 as mentioned before. There is no specific relation between these types, and the SMA braces don't have more priority in reducing the displacements than steel braces. Fig. 11 shows that the displacements of the deck level will be reduced for the El Centro accelerogram and will be increased for Kobe and Tabas accelerograms in the most time. However, SMA braces play a prominent role that they reduced the residual displacement of the structure. The maximum values of the deck level displacement which don't have any specific trend, and residual displacement which will be reduced by utilizing SMA braces in the five types of SPD12 are compared in Table 8.

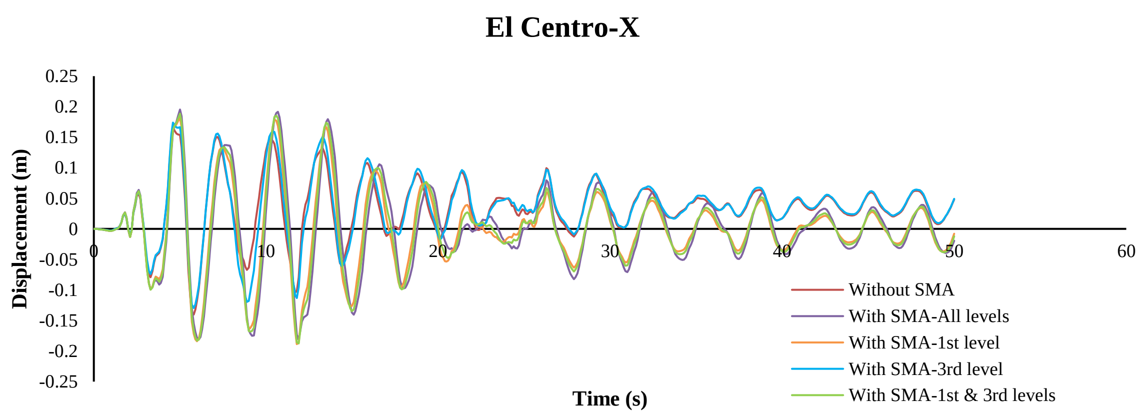

(a-1)

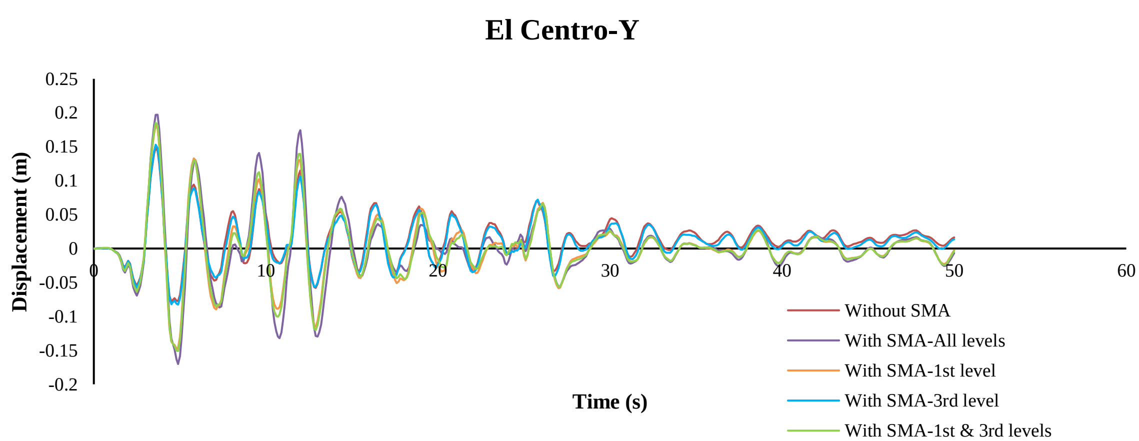

(a-2)

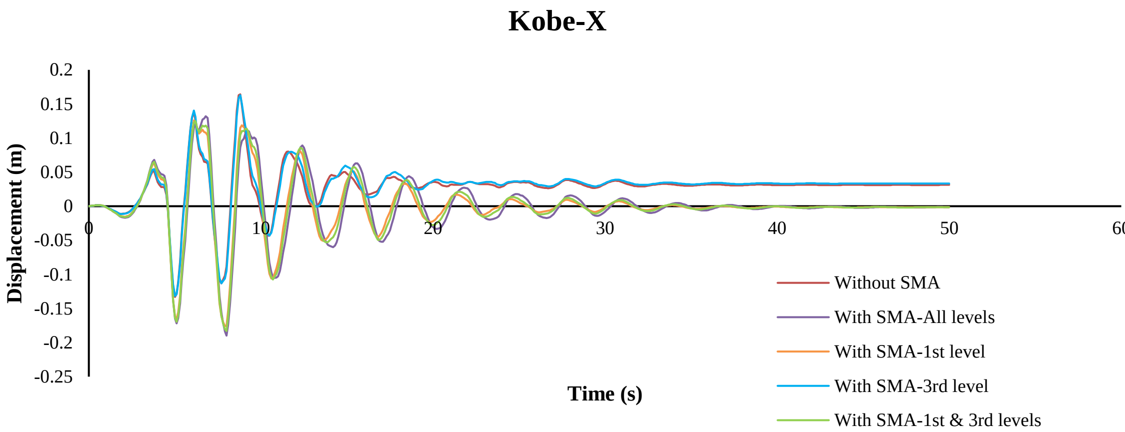
Kobe-X
Displacement (m)
0.2
0.15
0.1
0.05
0
-0.05
-0.1
-0.15
-0.2
-0.25
0
10
20
30
40
50
60
Time (s)
Without SMA
With SMA-All levels
With SMA-1st level
With SMA-3rd level
With SMA-1st & 3rd levels

(b-1)

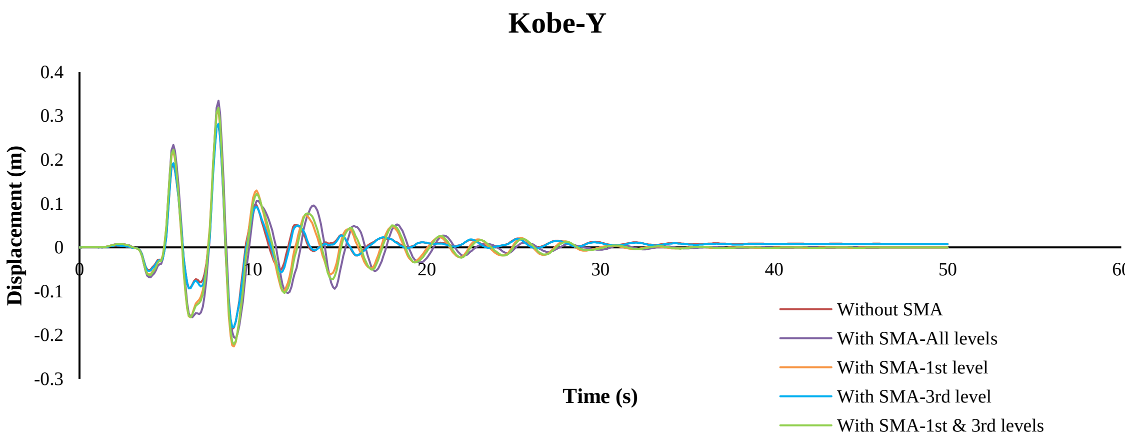
Kobe-Y
Displacement (m)
0.4
0.3
0.2
0.1
0
-0.1
-0.2
-0.3
0
10
20
30
40
50
60
Time (s)
Without SMA
With SMA-All levels
With SMA-1st level
With SMA-3rd level
With SMA-1st & 3rd levels

(b-2)

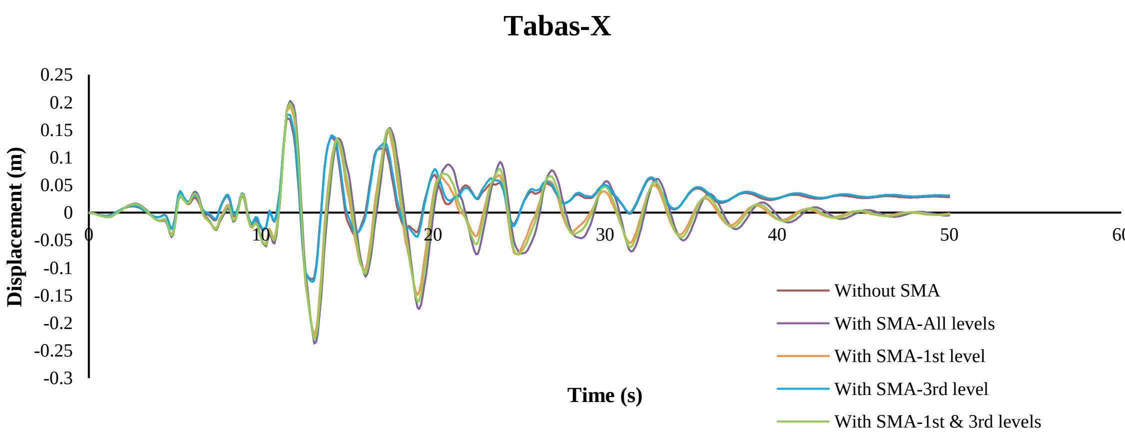
Tabas-X
Displacement (m)
0.25
0.2
0.15
0.1
0.05
0
-0.05
-0.1
-0.15
-0.2
-0.25
-0.3
0
10
20
30
40
50
60
Time (s)
Without SMA
With SMA-All levels
With SMA-1st level
With SMA-3rd level
With SMA-1st & 3rd levels

(c-1)

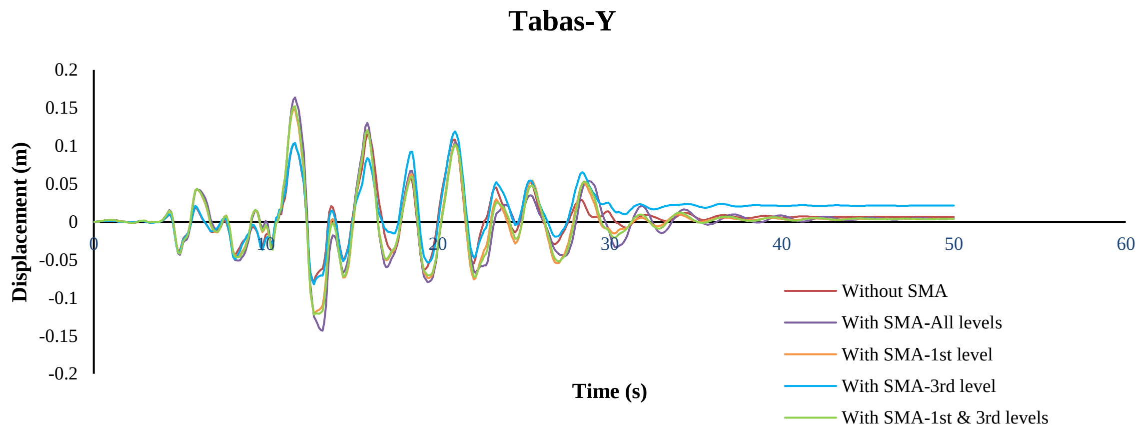

(c-2)

Fig. 11 The time history of displacement of the deck level of five types of SPD12 under the earthquake records of (a) El Centro, (b) Kobe, and (c) Tabas in two directions.

Table 8 The effect of SMA braces on the displacement and residual displacement of the deck level of SPD12

Earthquake	Deck level's maximum displacement (m)					Deck level's maximum residual displacement (m)				
	Without SMA	SMA in 1st level	SMA in 3rd level	SMA in 1st & 3rd levels	SMA in all levels	Without SMA	SMA in 1st level	SMA in 3rd level	SMA in 1st & 3rd levels	SMA in all levels
El Centro-X	0.163	0.179	0.184	0.178	0.175	0.024	0.000	0.025	0.000	0.000
El Centro-Y	0.143	0.165	0.140	0.161	0.166	0.050	0.001	0.049	0.001	0.001
Kobe-X	0.176	0.138	0.178	0.142	0.145	0.018	0.001	0.019	0.001	0.001
Kobe-Y	0.303	0.257	0.297	0.249	0.258	0.048	0.000	0.049	0.000	0.000
Tabas-X	0.186	0.189	0.185	0.188	0.185	0.018	0.002	0.018	0.002	0.002
Tabas-Y	0.103	0.133	0.105	0.130	0.134	0.022	0.003	0.028	0.003	0.003

The base shear comparison of the five types of SPD12 platform models shows that there is no relation between base shear and utilizing SMA braces, just like displacement comparison results. However, SMA braces due to their characteristics will reduce the residual base shear which will reduce the element residual internal forces and lower the side effects of fatigue in the structure. Fig. 12 shows the time history of the base shear for the five types of SPD12 platform subjected to the accelerograms of El Centro, Kobe, and Tabas earthquakes.

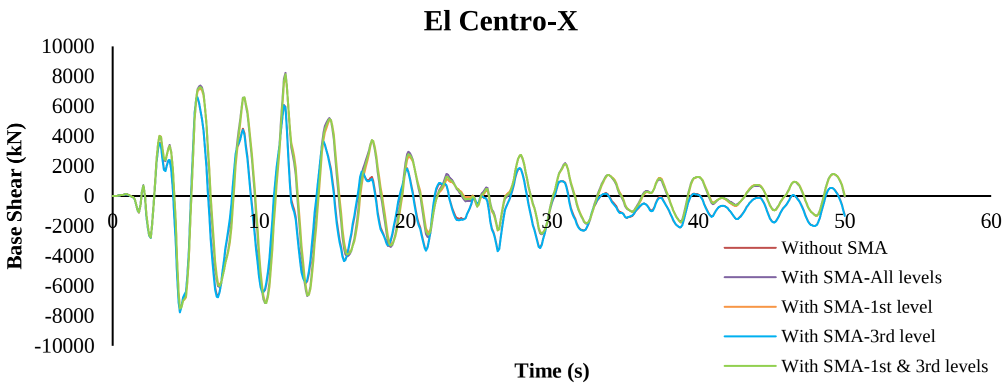
El Centro-X
Base Shear (kN)
10000
8000
6000
4000
2000
0
-2000
-4000
-6000
-8000
-10000
0
10
20
30
40
50
60
Time (s)
Without SMA
With SMA-All levels
With SMA-1st level
With SMA-3rd level
With SMA-1st & 3rd levels

(a-1)

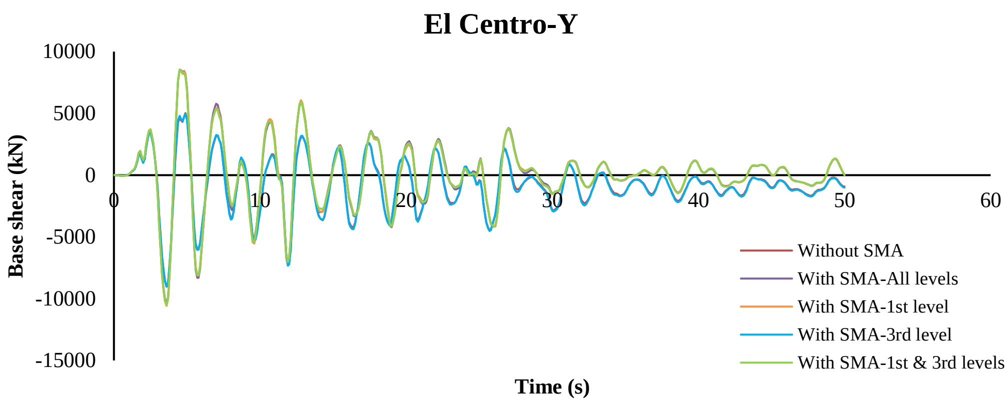
El Centro-Y
Base shear (kN)
10000
5000
0
-5000
-10000
-15000
0
10
20
30
40
50
60
Time (s)
Without SMA
With SMA-All levels
With SMA-1st level
With SMA-3rd level
With SMA-1st & 3rd levels

(a-2)

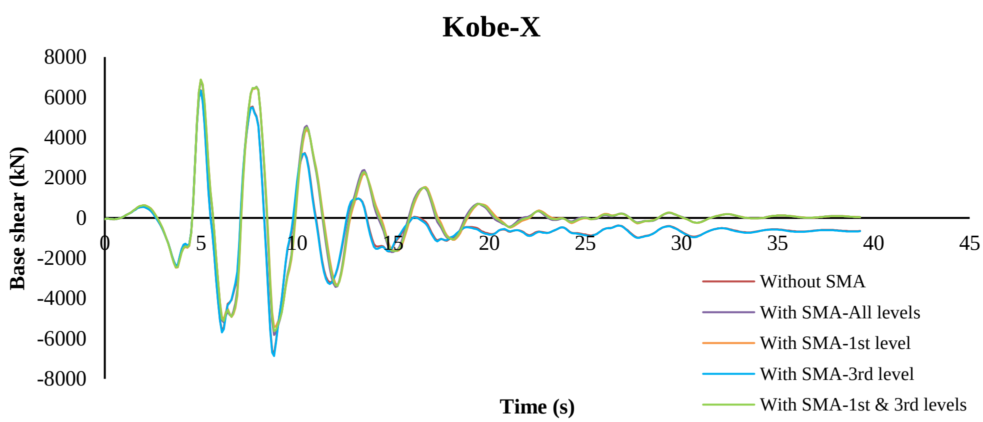
Kobe-X
Base shear (kN)
8000
6000
4000
2000
0
-2000
-4000
-6000
-8000
0
5
10
15
20
25
30
35
40
45
Time (s)
Without SMA
With SMA-All levels
With SMA-1st level
With SMA-3rd level
With SMA-1st & 3rd levels

(b-1)

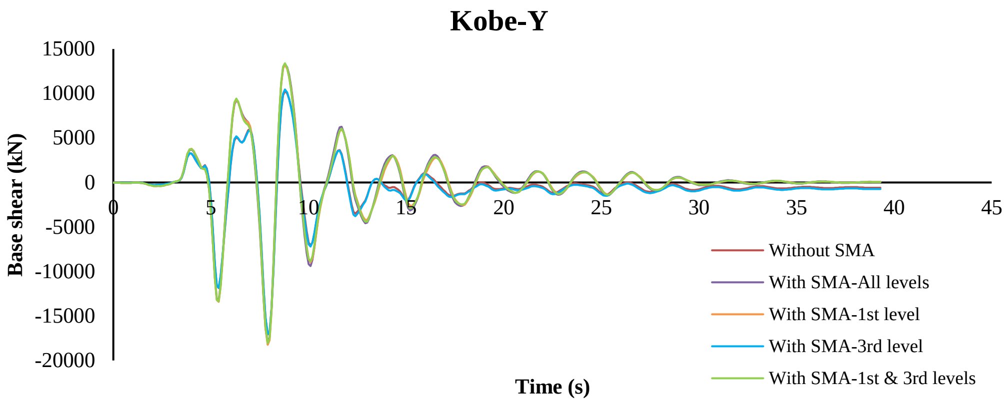

(b-2)

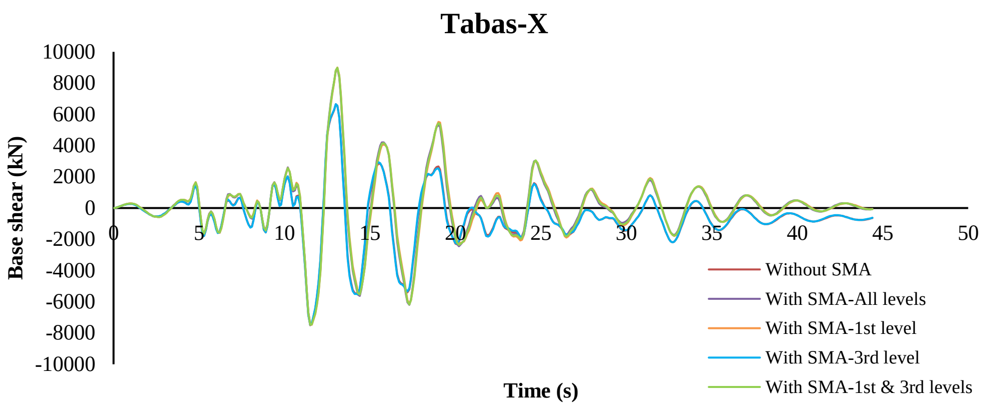

(c-1)

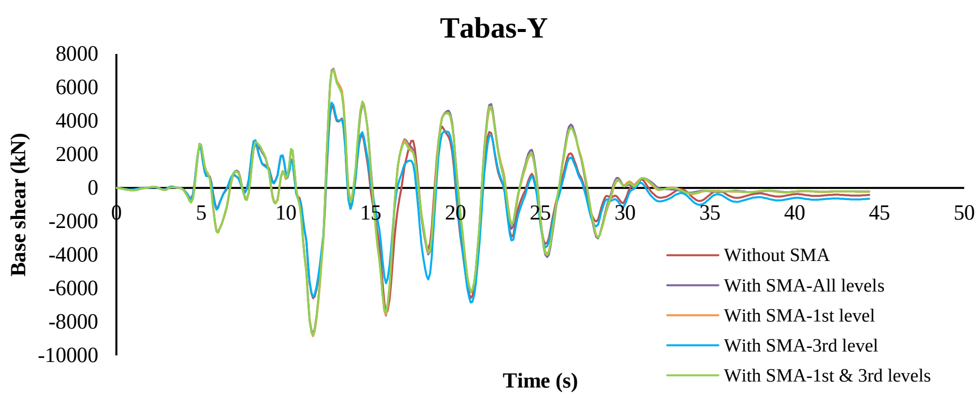

(c-2)

Fig. 12 The time history of the five types of platform's base shear under the earthquake records of (a) El Centro, (b) Kobe, and (c) Tabas in two directions.

The rigidity of the structure doesn't allow elements to experience the nonlinearity when they are subjected to the earthquake records. So, most of the elements are linear, and SPD12 doesn't have experienced a big displacement to be controlled by SMA bars.

3.3. The effect of SMA braces on pushover curve of the structure

For obtaining the effects of SMA braces on offshore platforms, SPD12 is pushed by modal pattern loading for experiencing 2m displacement at the deck level of the platform. Pushover curves of five types of SPD12 in two directions are shown in Fig. 13. By utilizing SMA braces, the structure will be under a greater force as the base shear increases when the structure goes through the nonlinear part. Therefore, deck displacement of SPD12 will be decreased if it is reinforced by SMA braces.

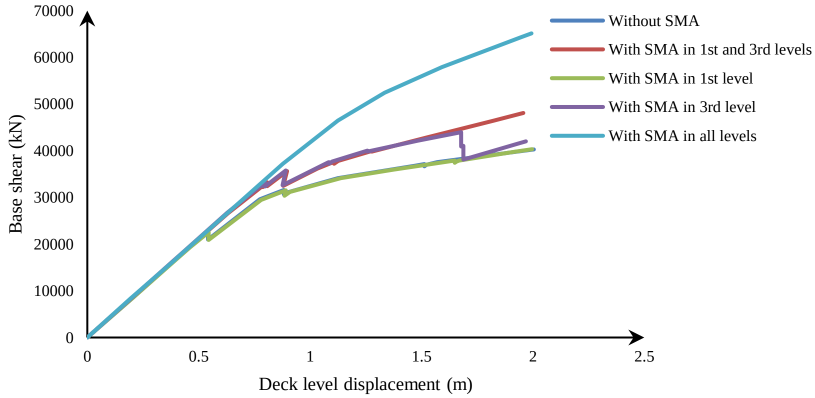

(a)

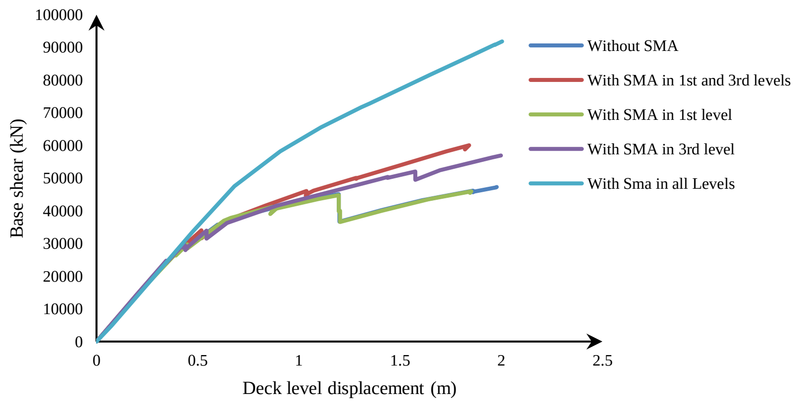

(b)

Fig. 13 Pushover curves of five types of SPD12; (a) X-direction, and (b) Y-direction

5. Conclusions

This study proposed utilizing SMA bars in jacket-type offshore platforms and assessed it for further designation of platforms. Due to the characteristics of SMA bars which resist only tensional forces, a novel connection is introduced to use SMA bars, just under tensional forces, in tubular braces. A seismic assessment of the platform is considered to obtain distribution of plastic hinges due to pushover analysis and optimization of using SMA bars in tubular braces was conducted. As a case study, an existing 4-legged jacket-type platform SPD12 was assessed with FEMA-356. As the results show, SMA bars have a little effect on the SPD12 that just reducing residual displacements, and it seems that utilizing SMA bars isn’t an appropriate solution. However, The SPD12 is very rigid and doesn't experience the nonlinearity in its structure subjected to considered accelerograms. So, for obtaining real effects of the SMA bars on structure, pushover analyses are conducted, and pushover curves of the five types of SPD12 are compared. This research shows that:

- For obtaining more effective offshore platform equipped with SMA braces, SMA braces have to be at least in first and third level of the structure to control the damage distribution and reduce the residual displacement.
- SMA braces can reduce residual displacement and stress in the structure, so the lifetime of the structure will be increased.
- Forces in elements and connections will be reduced about 85% by SMA braces. Therefore, API recommendations for design of the offshore platform can be improved.
- Reduction of deck level displacement and base shear can be obtained by SMA braces.
- Higher offshore platforms equipped with SMA braces can be designed in deeper sea efficiently and financially.

Declaration of interest

The authors report no conflicts of interest. The authors alone are responsible for the content and writing of this article.

References

[1] Hedayati Dezfuli F, Alam S.M. Shape memory alloy wire-based smart natural rubber bearing. Smart Materials and Structures 2013;22(4):045013.
[2] Alam M.S, Youssef M.A, Nehdi M. Utilizing shape memory alloys to enhance the performance and safety of civil infrastructure: a review. Canadian Journal of Civil Engineering 2007; 34(9):1075-86.
[3] Dolce M, Cardone D, Marnetto R. Implementation and testing of passive control devices based on shape-memory alloys. Earthquake Engineering and Structural Dynamics 2000; 29(7):945-68.
[4] Dolce M, Cardone D. Mechanical behavior of shape memory alloys for seismic applications. 2: austenite NiTi wires subjected to tension. International Journal of Mechanical Sciences 2001;43:2657-77.
[5] DesRoches R, McCormick J, Delemont M. Cyclic properties of superelastic shape memory alloy wires and bars. Journal of the Structural Engineering 2004; 130:38-46.
[6] Hong-nan LI, Xiao-yu HE, Lin-sheng HUO. Seismic response control of offshore platform structures with shape memory ally dampers. China Ocean Engineering 2005; 19(2):185-94.
[7] Asgarian B, Moradi S. Seismic response of steel braced frames with shape memory alloy braces. Journal of Constructional Steel Research 2011; 67:65-74.
[8] Wilde K, Gardoni P, Fujino Y. Base isolation system with shape memory alloy device for elevated highway bridges. Engineering Structures 2000; 22(3):222-29.
[9] Desroches R, Smith B. Shape memory alloys in seismic resistant design and retrofit: A critical review of their potential and limitations. Journal of Earthquake engineering 2004; 8(3): 415-29.
[10] Tamai H, Miura K, Kitagawa Y, Fukuta T. Application of SMA rod to exposed-type column base in smart structural system. 13th World Conference on Earthquake Engineering, Vancouver, B.C., Canada 2004;1884.
[11] Haque A.R, Alam M.S. Hysteretic Behaviour of a Piston Based Self-centering (PBSC) Bracing System Made of Superelastic SMA Bars–A Feasibility Study. Structures 2017; 12:102-14.
[12] Ocel J, DesRoches R, Leon R.T, Hess W.G, Krumme R, Hayes J.R, Sweeney S. Steel Beam-Column Connections Using Shape Memory Alloys. Journal of Structural Engineering. 2004; 130(5): 732-40.
[13] Sepulveda J, Boroschek R, Herrera R, Moroni O, Sarrazin M. Steel beam-column connection using copper-based shape memory alloy dampers. Journal of Constructional Steel Research 2008; 64(4):429-35.
[14] Rofooei F.R, Farzaneh A.Y. Numerical study of an innovative SMA based beam-column connection in reducing the seismic response of steel MRF structures. Scientia Iranica 2016;23(5):2033-43.

[15] Jamalpour R, Nekooei M, Sarvghad Moghdam A. Seismic response reduction of steel MRF using SMA equipped innovated low-damag column foundation connection. Civil Engineering Journal 2017;3(1):1-14.
[16] Wu Z, He X, Zhang Y. Steel beam-to-column connections using martensite shape memory alloys. Advanced Materials Research 2011;243-249:662-665.
[17] Shabakhty N, Givkay A. Investigation on response of fixed offshore platforms equipped with shape memory alloy elements at different depth under extreme wave loading. Marine Engineering 2014;18:1-12.
[18] Aghajani Delavar M, Pahlavikhah Varnosfaderani M, Bargi K. Seismic response of a fixed jacket-type offshore platform equipped with shape memory alloy. 4th International Congress on Civil Engineering, Architecture and Urban Development, Shahid Beheshti University, Tehran, Iran 2016.
[19] Structural report of wellhead platform SPD12 (2010) South Pars Gas Field Development Phase 12. Report no. SP12-24-D-23-5-001/D3.
[20] SAP2000 (2004), V14.0-Integrated Software for Structural Analysis and Design, Computers and Structures Inc; Berkeley, United states.
[21] American Petroleum Institute (API) (2000), Recommended Practice for Planning, Design and Constructing Fixed Offshore Platforms: API Recommended Practice 2A (RP 2A), 21th ed.; Washington, United states.
[22] Lotfollahi-Yaghin MA, Ahmadi H, Tafakhor H. Seismic responses of an offshore jacket-type platform incorporated with tuned liquid dampers. Advances in Structural Engineering 2016;19(2):227-38.
[23] Toyama Y. Drift-wood Collision Load on Bow Structure of High-speed Vessels. Marine Structures 2009;22:24-41.
[24] Fugazza D. Shape memory alloy devices in earthquake engineering: mechanical properties, constitutive modeling and numerical simulations. Master's thesis. Pavia (Italy): European school for advanced studies in reduction of seismic risk; 2003.
[25] Bruno S, Valente C. Comparative response analysis of conventional and innovative seismic protection strategies. Earthquake Engineering and Structural Dynamics 2002;31:1067-92.
[26] Andrawes B, McCormick J, DesRoches R. Effect of cyclic modeling parameters on the behavior of shape memory alloys for seismic applications. Proceedings of SPIE 2004;5390:324-34.
[27] DesRoches R, McCormick J, Delemont M. Cyclic properties of superelastic shape memory alloy wires and bars. Journal of the Structural Engineering 2004;130:38-46.
[28] FEMA-356 (2000), Pre-standard and commentary for the seismic rehabilitation of buildings, Federal Emergency Management Agency; Washington, United states.
[29] Standard no. 360 (2012), Iranian code of instructions on seismic reconstruction of existing buildings, Building and Housing Research Center; Tehran, Iran.
[30] Aghajani Delavar M, Bargi K. Prediction of Local Seismic Damage in Jacket-type Offshore Platforms. AUT Journal of Civil Engineering 2018;2(2):241-50.
[31] Kari A. A new dual bracing system consisting of shape memory alloy braces and innovative braces. Ph.D. thesis. Tehran (Iran): University of Tehran; 2014.
[32] SeismoSignal 2016: A computer program for signal processing of time-histories. Available online from http://www.seismosoft.com.